DYNAMIC PORE WATER PRESSURE ACTING ON QUAY WALLS DURING EARTH-QUAKES

BY

Haruo MATUO* and Sukeo O-HARA**

ABSTRACT

In our previous paper we have reported that we could clearly observe the existence of dynamic pore water pressure of the saturated sand acting on the wall during vibration.

In this paper we are to report the following study on the dynamic pore pressure

(1) theoretical solution assuming the pore water as compressible.
(2) results of systematic experimental study.
(3) its relation to the dynamic sand pressure.
(4) some additional results obtained during experiment.

THEORETICAL SOLUTION OF DYNAMIC PORE PRESSURE ACTING ON THE WALL

In the following theoretical solution, it is assumed that the soil undergoes no deformation during vibration and that pore water flows through the pores, Darcy's formula being applied to the flow.

Navier-Stokes equation:-

$$\left.\begin{aligned} \frac{\partial u}{\partial t} &= -\frac{1}{\rho_w}\frac{\partial p}{\partial x} + \frac{1}{3}\nu\frac{\partial}{\partial x}\left(\frac{\partial u}{\partial x}+\frac{\partial v}{\partial y}\right) + \nu\nabla^2 u \\ \frac{\partial v}{\partial t} &= -\frac{1}{\rho_w}\frac{\partial p}{\partial y} + \frac{1}{3}\nu\frac{\partial}{\partial y}\left(\frac{\partial u}{\partial x}+\frac{\partial v}{\partial y}\right) + \nu\nabla^2 v \end{aligned}\right\} \quad (1)$$

Where u, v : horizontal and vertical velocity of pore water respectively
p : dynamic pore water pressure
ν : coefficient of dynamic viscosity of pore water
ρ_w : density of pore water

Equation of continuity:-

$$\frac{\partial u}{\partial x} + \frac{\partial v}{\partial y} = -\frac{1}{\rho_w}\frac{\partial \rho_w}{\partial t} \quad (2)$$

Equation of characteristics, taking K, bulk modulus of pore water.

$$\frac{1}{K}\frac{\partial p}{\partial t} = \frac{1}{\rho_w}\frac{\partial \rho_w}{\partial t} \quad (3)$$

Substituting (2) (3) into (1), we obtain

---

* Prof. Emeritus of Kyushu University Civil Engineering.
** Prof. of Yamaguchi University Civil Engineering.

$$\left.\begin{aligned}\frac{\partial u}{\partial t} &= \frac{1}{\rho_w}\frac{\partial}{\partial x}\left(-p+\frac{1}{3}\frac{\rho_w \nu}{\kappa}\frac{\partial p}{\partial t}\right)+\nu\nabla^2 u \\ \frac{\partial v}{\partial t} &= \frac{1}{\rho_w}\frac{\partial}{\partial y}\left(-p+\frac{1}{3}\frac{\rho_w \nu}{\kappa}\frac{\partial p}{\partial t}\right)+\nu\nabla^2 v\end{aligned}\right\} \tag{4}$$

Except when the period of vibration is very small, $\frac{1}{3}\frac{\rho_w \nu}{\kappa}\frac{\partial p}{\partial t}$ is negligibly small.

Let u_*, v_* : relative velocity of pore water to the soil particles
λ : porosity of the soil
k : coefficient of permeability
g : accerelation of gravity

By applying Darcy's law,

$$\nu\nabla^2 u = \frac{-\lambda g}{k}u_* , \quad \nu\nabla^2 v = \frac{-\lambda g}{k}v_*$$

from which

$$\left.\begin{aligned}\frac{\partial u}{\partial t} &= -\frac{1}{\rho_w}\frac{\partial p}{\partial x}-\frac{\lambda g}{k}u_* \\ \frac{\partial v}{\partial t} &= -\frac{1}{\rho_w}\frac{\partial p}{\partial y}-\frac{\lambda g}{k}v_*\end{aligned}\right\} \tag{5}$$

Equation (5) is the equation of pore water movement

From eq. (2) and eq. (3),

$$\frac{\partial p}{\partial t} = -\kappa\left(\frac{\partial u}{\partial x}+\frac{\partial v}{\partial y}\right) \tag{6}$$

Boundary conditions:-

$$\text{(i)}\ (u)_{x=0}=(u)_{x=a}=-\frac{\alpha g}{\omega}\sin\omega t, \quad \text{(ii)}\ (v)_{y=0}=0, \quad \text{(iii)}\ (p)_{y=H}=0$$

Where α : Seismic coefficient i.e.,max. acceleration of earthquakes divided by acceleration of gravity.

Further, let ξ, η : compornents of relative displacememt for x-y-direction.

Thus,

$$\frac{\partial u}{\partial t}=\frac{\partial^2 \xi}{\partial t^2}-\alpha g\cos\omega t, \quad \frac{\partial v}{\partial t}=\frac{\partial^2 \eta}{\partial t^2}, \quad u_*=\frac{\partial \xi}{\partial t}, \quad v_*=\frac{\partial \eta}{\partial t}$$

eq. (5) and (6) are changed to following eq. (7) and (8):

$$\left.\begin{aligned}\frac{\partial^2 \xi}{\partial t^2} &= -\frac{1}{\rho_w}\frac{\partial p}{\partial x}-\frac{\lambda g}{k}\frac{\partial \xi}{\partial t}+\alpha g\cos\omega t \\ \frac{\partial^2 \eta}{\partial t^2} &= -\frac{1}{\rho_w}\frac{\partial p}{\partial y}-\frac{\lambda g}{k}\frac{\partial \eta}{\partial t}\end{aligned}\right\} \tag{7}$$

$$p = -\kappa\left(\frac{\partial \xi}{\partial x} + \frac{\partial \eta}{\partial y}\right) \tag{8}$$

Boundary conditions:-

(i) $(\xi)_{x=0} = (\xi)_{x=a} = 0$, (ii) $(\eta)_{y=0} = 0$, (iii) $(p)_{y=H} = 0$

From eq. (7) and (8), we obtain following equation

$$-\frac{1}{\kappa}\frac{\partial^2 p}{\partial t^2} = -\frac{1}{\rho_w}\left(\frac{\partial^2 p}{\partial x^2} + \frac{\partial^2 p}{\partial y^2}\right) + \frac{\lambda g}{k\kappa}\frac{\partial p}{\partial t} \tag{9}$$

Boundary conditions

(i) $\left(\frac{\partial p}{\partial x}\right)_{x=0} = \rho_w \alpha g \cos\omega t \quad (\because \xi = 0)$

(ii) $\left(\frac{\partial p}{\partial x}\right)_{x=a} = \rho_w \alpha g \cos\omega t \quad (\because \xi = 0)$

(iii) $\left(\frac{\partial p}{\partial y}\right)_{y=0} = 0 \quad (\because \eta = 0)$

(iv) $(p)_{y=H} = 0$

The solution of eq. (9) is easily obtained and we have as the dynamic pore pressure $(p)_{x=0}$ which acts on the wall as follows:-

$$(p)_{x=0} = \sum_{n=0}^{\infty} (-1)^n \frac{4\rho_w \alpha g H}{(2n+1)\pi} \cos\frac{(2n+1)\pi}{2}\xi \left[\left(\cosh\gamma_n\frac{a}{H} - \cos\delta_n\frac{a}{H}\right)\right.$$

$$\times\left\{-\sinh\gamma_n\frac{a}{H}(\gamma_n\cos\omega t + \delta_n\sin\omega t) + \sin\delta_n\frac{a}{H}(\gamma_n\sin\omega t - \delta_n\cos\omega t)\right\}\Big]$$

$$\times \frac{1}{(\gamma_n^2+\delta_n^2)\left(\sinh^2\gamma_n\frac{a}{H}\cdot\cos^2\delta_n\frac{a}{H} + \cosh^2\gamma_n\frac{a}{H}\cdot\sin^2\delta_n\frac{a}{H}\right)} \tag{10}$$

$$\begin{matrix}\gamma_n \\ \delta_n\end{matrix} = \sqrt{\frac{\pm\left[\left(\frac{(2n+1)\pi}{2}\right)^2 - \left(\frac{\rho_w\omega^2H^2}{\kappa}\right)\right] + \sqrt{\left[\left(\frac{(2n+1)\pi}{2}\right)^2 - \left(\frac{\rho_w\omega^2H^2}{\kappa}\right)\right]^2 + \left(\frac{\rho_w\lambda g\omega H^2}{\kappa k}\right)^2}}{2}}$$

in which $\xi = y/H$

Putting $a \to \infty$ in Formula (10), we have

$$(p)_{x=0} = \sum_{n=0}^{\infty} \frac{(-1)^{n+1}4\rho_w\alpha g H}{(2n+1)\pi}\cos\frac{(2n+1)\pi}{2}\xi\,\frac{(\gamma_n\cos\omega t + \delta_n\sin\omega t)}{(\gamma_n^2+\delta_n^2)} \tag{11}$$

The dynamic pore water pressure against quay walls during earthquakes, can be caluculated according to Formula (11).

Now a result of caluculation of the dynamic pore pressure against quay walls is shown in Fig. 2, in dimensionless expression, taking the back-filling soil of the wall as sand, and between the range of

$k = 10^{-3} \sim 1.0$ cm/sec, $\omega = 10\pi \sim \pi$, $H = 5 \sim 15$ m,

in which P is the total force acting on the wall

T : Period of forced vibration.

δ/T : Phase difference.

H : Height of the wall.

From Fig. 2, we see that when $\rho_w\lambda g\omega H^2/\kappa k \leq 1$

the dynamic pore pressure is nearly equal to that of Westergaard and there is no phase difference between the forced vibration and pressure.

From Fig.2, we obtain the value of dynamic pore pressure acting on quay walls, i.e., resultant force and point of application for the wide range of $\rho_w \lambda g \omega H^2 / \kappa k$.

For example, taking $H = 7$m, $\lambda = 0.5$, $k = 10^{-2}$ cm/s, $T = 2.0$ s we have from Fig.2 $\rho_w \lambda g \omega H^2 / \kappa k = 3.77$ and max. value of the resultant force $P = 0.34 \rho_w \alpha g H^2$. This value corresponds to 70 % of Westergaard's value. Also the phase difference in this case is $\delta = 0.04T$.

EXPERIMENTS ON SATURATED SAND

Our experiment was carried out using a steel box filled with sand saturated with water. The box which has the dimensions 30(height)×60(width)×100 cm(length) was placed on the shaking table.

The dynamic pressure was measured at the end of the box with the pressure cells.

During this experiment we observed the following characteristics of the cells,i.e., the relation of the rigidity of the cell-membrane and the observed pressure: when we use a cell-membrane of normal type with larger flexibility, the increase of pore water pressure causes the deformation - increase of the membrane, and this causes soil pressure-decrease,thus unable to observe actual pore pressure change.

And we also have ascertained that we can make tolerably good observation using less-flexible membrane, i.e., under the flexibility Δ/R less than 0.15×10^{-2} cm^2/kg.

in which Δ : the deformation of the membrane at center per unit pressure
R : Radius of the membrane.

On the other hand, pure dynamic pore pressure was measured by pressure cells having a screen before the membrane.

Fig. 3 showns the results obtained using these cells.

Here vertical co-ordinate is the positive half amplitude of dynamic pressure, taking the third series of vibration after filling. Because by the first and second series of vibration the sand settles down almost to its final state.

The period of forced vibration was about 0.3 sec and the coeff. of permeability of the sand was 0.19 cm/sec.

From Fig. 3, we have following conclusions:-

(1) The dynamic pore pressure-increase (of positive half amplitude) is nearly equal to values calculated according to Formula (10).

(2) The dynamic pressure of water saturated sand is nearly equal to the sum of the pore water- and the sand-pressure.

By the next experiment, we have measured the dynamic pore pressure at various sites in the sand with the pressure cell as shown in Fig. 4.

Fig. 5 is the records of the dynamic pore pressure at the depth d=15 cm . As may be seen in Fig. 5, the wave pattern at $l = 0$ and $l = 50$ cm is very different. By examining these records, we have concluded that the deformation of the wave is caused by the periodic negative pore pressure due to dilatancy, which is caused by the swelling of sand,

occuring every half period of the forced vibration. The deformed wave is the compound of the dynamic pore pressure and the negative pore pressure.

Fig. 6 illustrates the reason why such irregular forms of pressure occurs.

We have calculated the amplitudes x and y by the formula shown in Fig. 6, from the pressure records of Fig. 5, and a result is shown in Fig. 7. This coincides with our theoretical result.

The horizontal distribution of the amplitude of dynamic pore pressure is similar to the result obtained by formula (10).

The horizontal distribution of negative pore pressure is similar to that of shearing strain in sand due to vibration, except at the depth $d = 5$ cm. This discrepancy at $d = 5$ cm may be explained it is due to the vibrating motion of the surface water wave, and this disturbs the occurance of the dilatancy.

EFFECT OF THE RIGIDITY OF PRESSURE CELLS ON THE PORE PRESSURE

In Fig. 8, a and b are the total amplitudes of pressure measured at the wall by flexible pressure cell without the screen. a is of saturated sand, and b is of drained wet sand. Broken line c is the total amplitude of pore pressure measured by the cell with the screen.

The flexibility of the cell Δ/R used for this experiment was 0.28×10^{-2} cm^2/kg in which Δ is the deformation and R is the radius of the membrane of the cell.

At first thought the sum of two amplitudes of b and c seem to be equal to a. But the result of previous experiment was not in accordance with it. The values of $b+c>a$.

The reason of this discrepancy was experimentally pursued, and we could conclude that it is due to the considerable amount of flexibility of the membrane of the cell. The experimental apparatus for this purpose was shown in Fig. 9.

It is cylindlical compression apparatus, in which the pressure cell to be tested is fixed at the bottom of the cylinder. The cell undergoes the pressure transmitted to the sand from the upper porous loading plate, as well as the pore air pressure from the air chamber which is transmitted through the void of the porous plate.

The experiment was carried out as follows: After filling the sand in the chamber, the vertical pressure was kept $\sigma_v = 0.1$ kg/ cm^2, for the first time, and the pore pressure was increased stepwise in static experiment. In dynamic experiment, the pore pressure was changed periodicaly by the apparatus as shown in Fig. 11., and the record of the pressure cell was taken by pen-recorder.

Next under $\sigma_v = 0.2$ and 0.3 kg /cm^2 , the same record was taken.

For this test, 9 pressure cells with different radii and rigidities were tested and 4 kinds of sand (Fig. 10) with different grain-size were used.

Fig. 12 shown an example of the records obtained by the experiment.

This shows 3 different amplitudes under the same pore pressure change with different ($\sigma_v = 0.1$, 0.2, and 0.3 kg/ cm^2). The amplitude of the cell-reading(strain of membrane) is inversely proportional to the sand pressure.

Fig. 13 (a) (b) are the results of this experiment, in which measured values are smaller than the values to be expected, i.e., the air pressure (standerd value).

By examining these results, we found that the difference between the measured and standerd values depend on the flexibility of membrane, and sand pressure σ_v , where standerd value means the measured values obtained without sand in the chamber.

Now taking $\cot\theta/\cot\theta_A$ (Fig. 14)—— where $\cot\theta$: tangential gradient of measured curve and $\cot\theta_A$: that of standerd curve —— we observed its relation to Δ/R and σ_v (Fig. 15) .

From these figures we could conclude that Δ/R should be less than 0.15×10^{-2} cm^2/kg so as we can make good measurment.

CONCLUSION

Our conclusions on the excess earth and pore pressure of water saturated soil during earthquakes are as follows:

(1) Dynamic pore pressure should be considered apart from earth pressure for the design of quay walls.

(2) According to our theoretical calculation the dynamic pore pressure ——resultant force and point of application acting on quay walls are as shown in Fig. 2 .

(3) Quay walls undergoes the excess pressure consisting of the excess earth pressure plus excess dynamic pore pressure.

(4) Additional results obtained: -

a) Examining the irregular pressure curves in saturated sand during vibration, we could make matters clear by assuming periodic negative pore pressure due to dilatancy of sand mass.

b) The effect of the rigidity of pressure-cell-membrane which has been hitherto overlooked was made clear by our experiment.

BIBLIOGRAPHY

Matuo, H & O-hara, S. "Lateral Earth Pressure and Stability of Quay Walls during Earthquakes" Proc. of 2nd WECC .

O-hara, S. " Dynamic Pore Pressure exerted to a Vertical Wall" Trans. J.S.C.E. No 87, 1962 .

O-hara, S. " Experimental Study of Dynamic Pressure of Water Saturated Sand" Trans. J.S.C.E. No 99, 1963 .

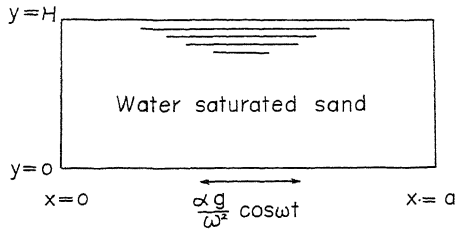

Fig. 1

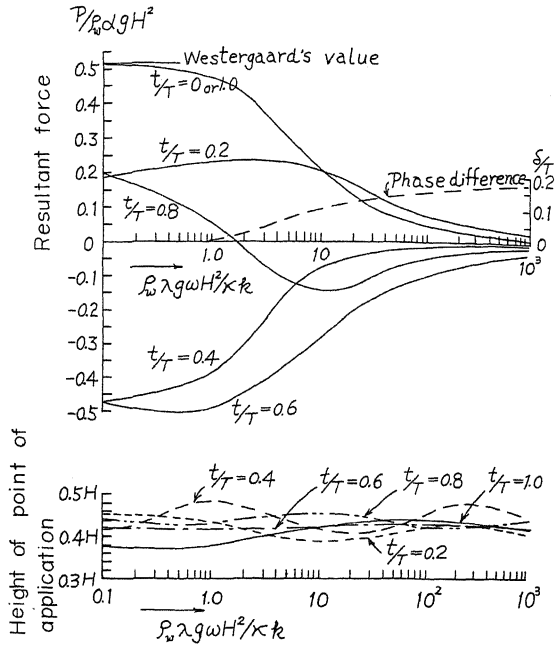

Fig.2. Computed resultant force and the point of application of the dynamic pore pressure

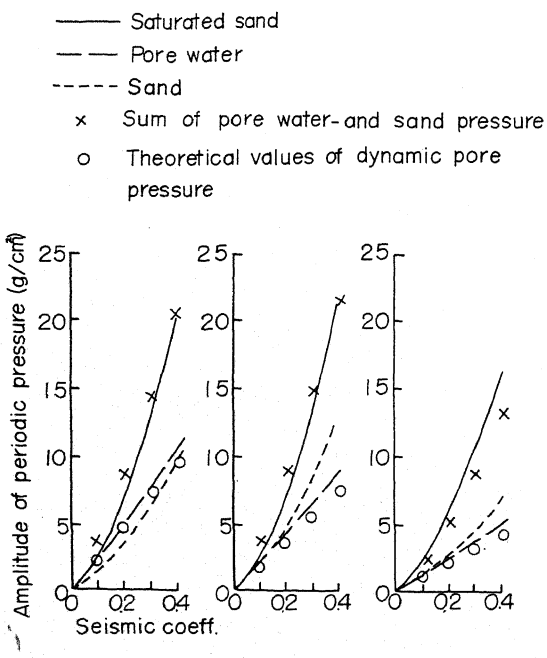

Fig.3 Amplitude of dynamic pressure

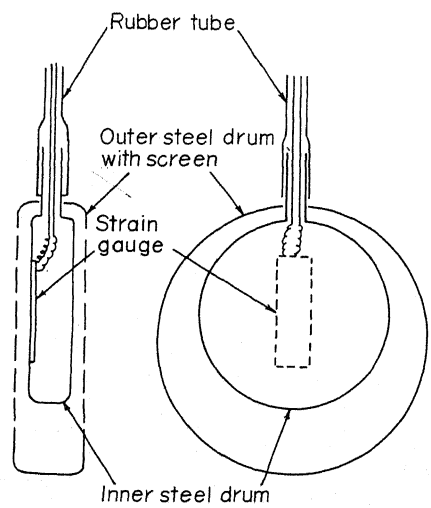

Fig.4. Pore pressure cell buried in sand

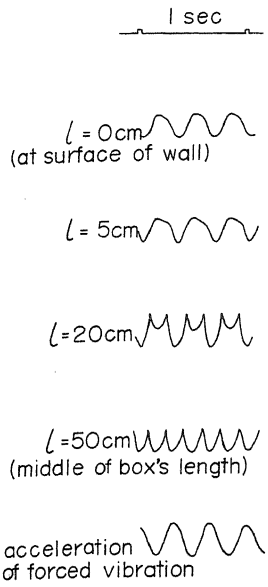

Fig.5 Record of dynamic pore water pressure

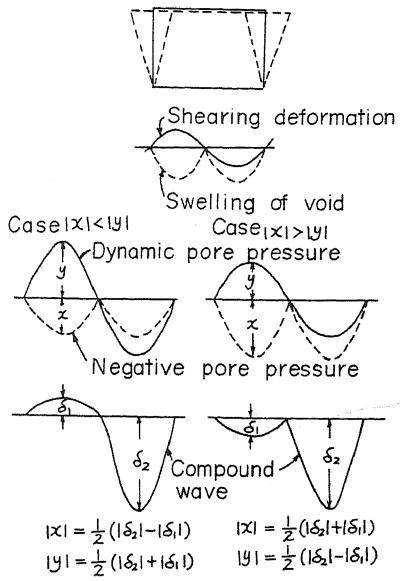

Fig.6 Explanation of irregularity of dynamic pore pressure

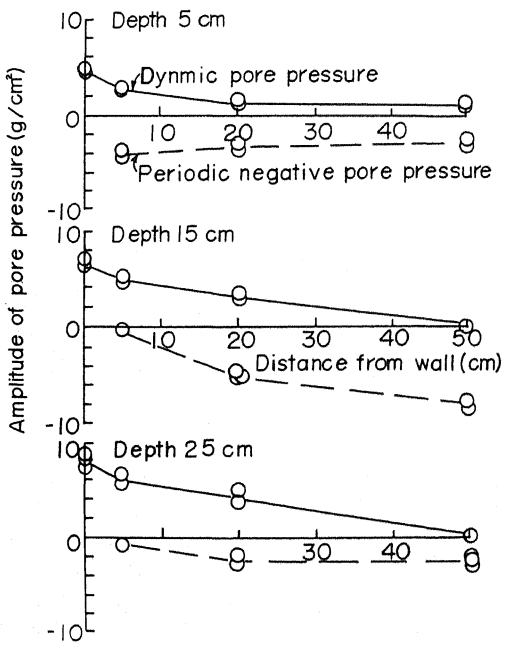

Fig.7 Horizontal distribution of pore pressure (at seismic coeff.= 0.3)

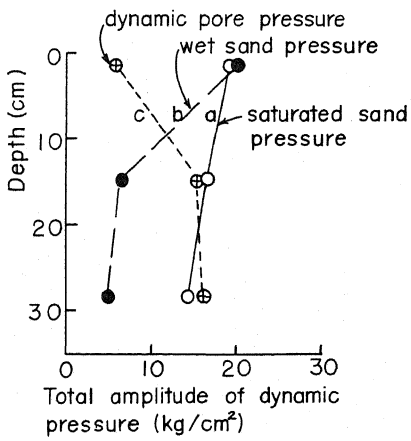

Fig. 8 Vertical distribution of dynamic pressure

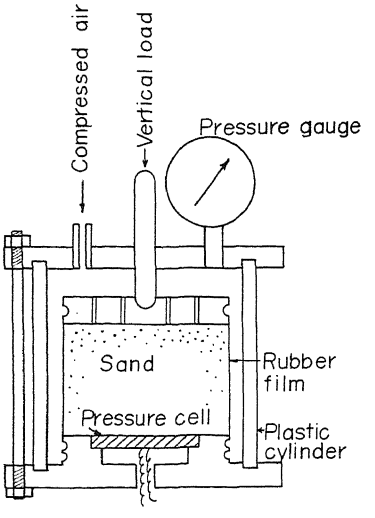

Fig.9 Calibration apparatus for pressure cell

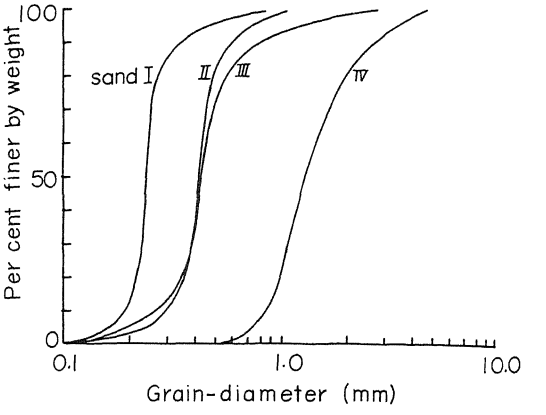

Fig.10 Grain-size distribution curve

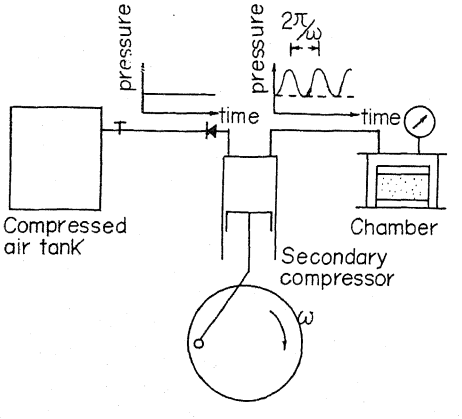

Fig.11 Equipment to give periodical change of chamber-pressure

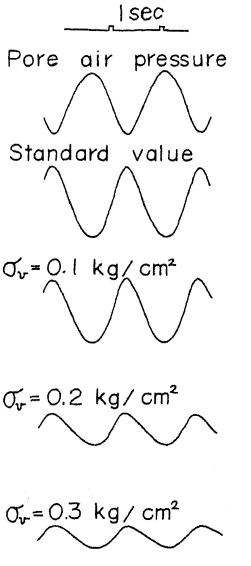

Fig.12 Record of pressure cell under different σ_v

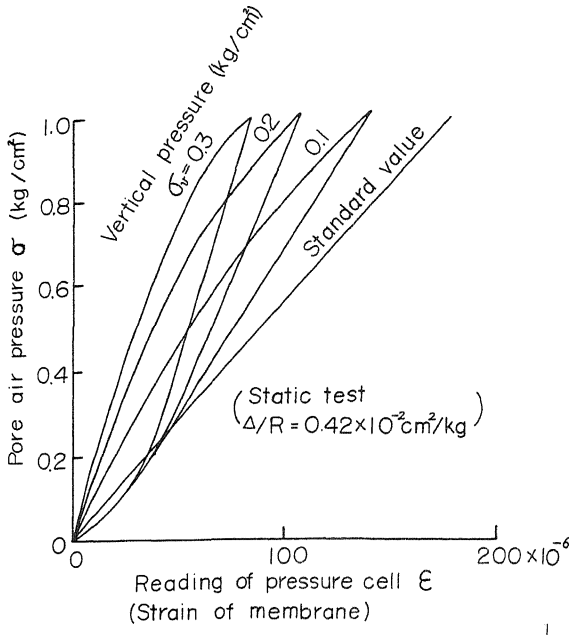

Fig. 13(a) σ-ε diagram

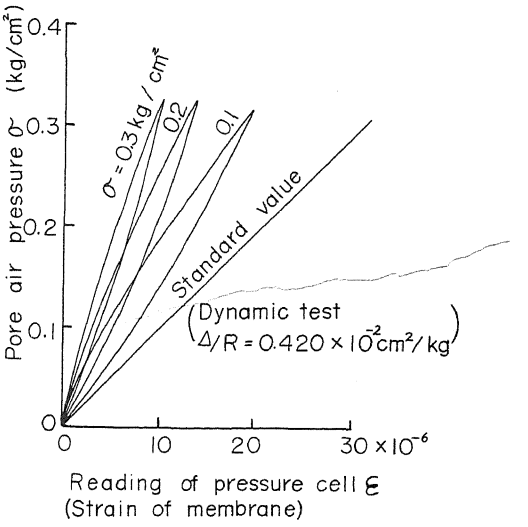

Fig. 13(b) σ-ε diagram

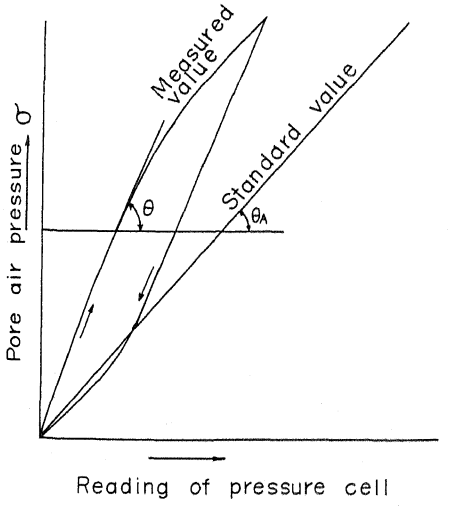

Fig. 14

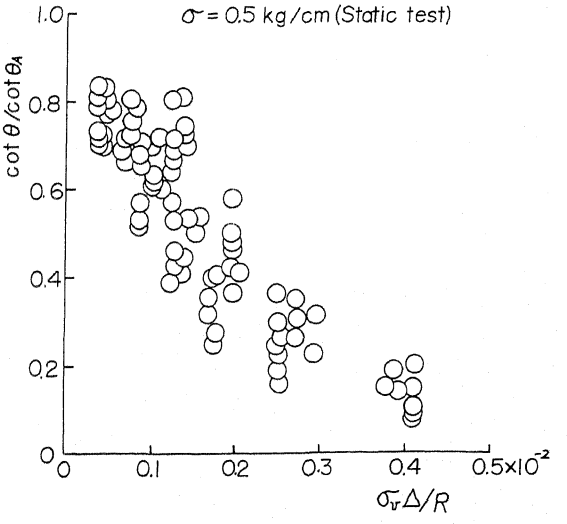

Fig. 15, (a) $\sigma_v\Delta/R$ - $\cot\theta/\cot\theta_A$ diagram

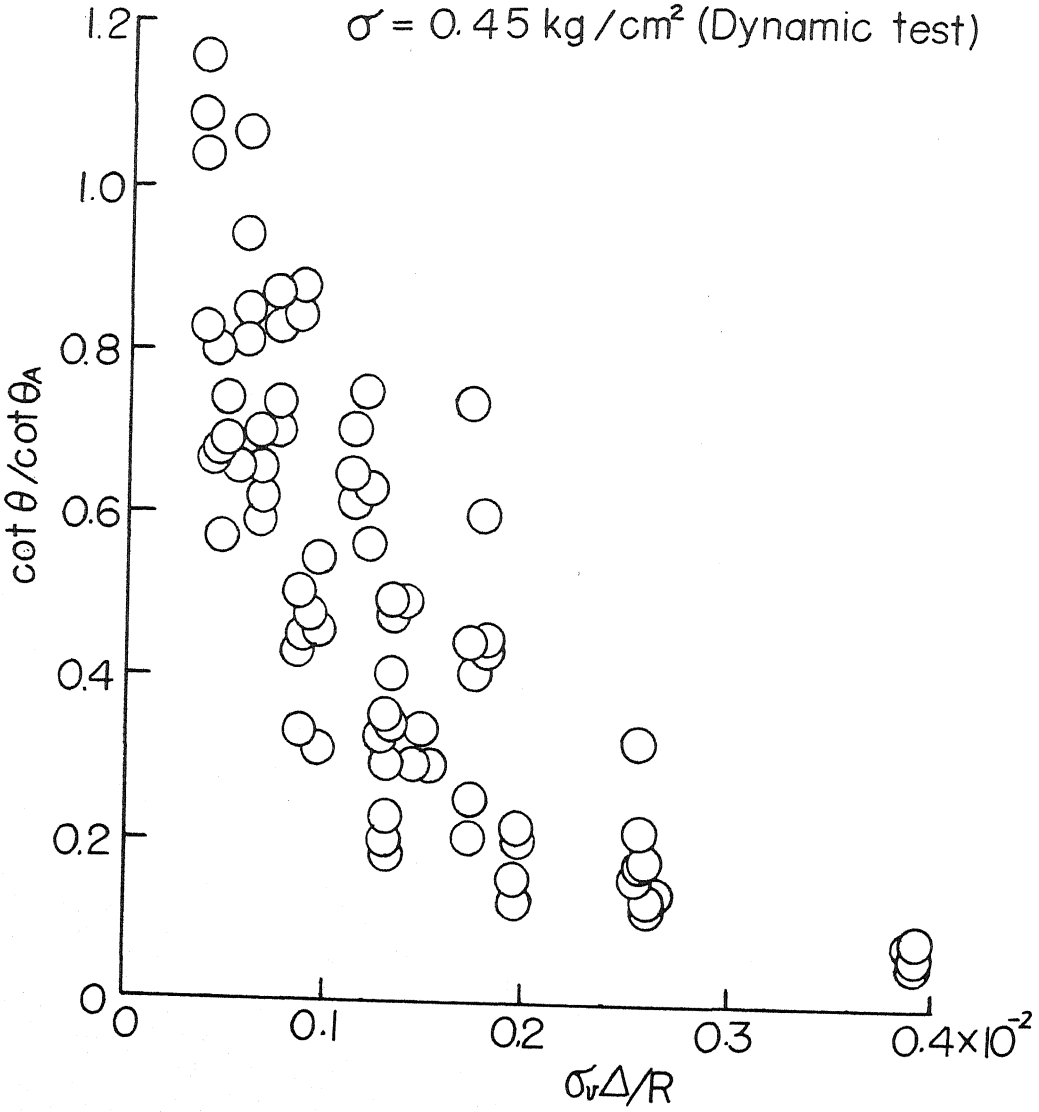

Fig. 15(b) $\sigma_v\Delta/R$ $\cot\theta/\cot\theta_A$ diagram

DYNAMIC PORE WATER PRESSURE ACTING ON QUAY WALLS DURING EARTHQUAKES

BY: H. MATUO AND S. OHARA

QUESTION BY: A. TORK - NEW ZEALAND

1. Refer to Fig. 3: three cases are shown - would the author please explain what these cases are for. Are they for different depths?

2. Refer to Fig. 8: What is the difference between "wet" and "saturated" sand pressures? Why are the "wet sand" + "dynamic pore" pressures not equal to "saturated sand" pressures as was shown in Figure 3? Is Figure 8 prepared for a seismic coefficient of $\alpha = 0.3$?

3. I assume that all pressures shown in figures 3, 7 & 8 are for dynamic fluctuations only, and do not include static pressure.

   Could the authors please indicate the static lateral pressure on container walls for the sand used in the experiments. What was the density and the angle of internal friction for the sand used?

AUTHORS' REPLY:

1. Fig. 3 shows the results at three different depths from the sand surface (from left to right 5 cm, 15 cm, 25 cm respectively).

2. The reason why the "wet sand" + "dynamic pore" pressure are not equal to "saturated sand" pressure (referring Fig. 8), is due to the rather large flexibility of the pressure cell used in Fig. 8.

   The "saturated sand" pressure obtained by these cells became smaller than the sum of "wet sand" pressure and "dynamic pore" pressure. The flexibility of Fig. 8 being $\Delta/R = 0.28 \times 10^{-2} cm^2/kg$ and that of Fig. 3 being $\Delta/R = 0.11 \times 10^{-2} cm^2/kg$. This was also explained in the original paper (in the middle of p. 4).

3. All pressures shown in Fig. 3, 7 & 8 are dynamic pressure only and do not include static pressures. The mean values of static pressures are shown in the following figure here.

   The apparent density of the sand used in this experiment is 1.35 g/cm^3 and the specific gravity is 2.62. The angle of internal friction is 41.4 degrees.

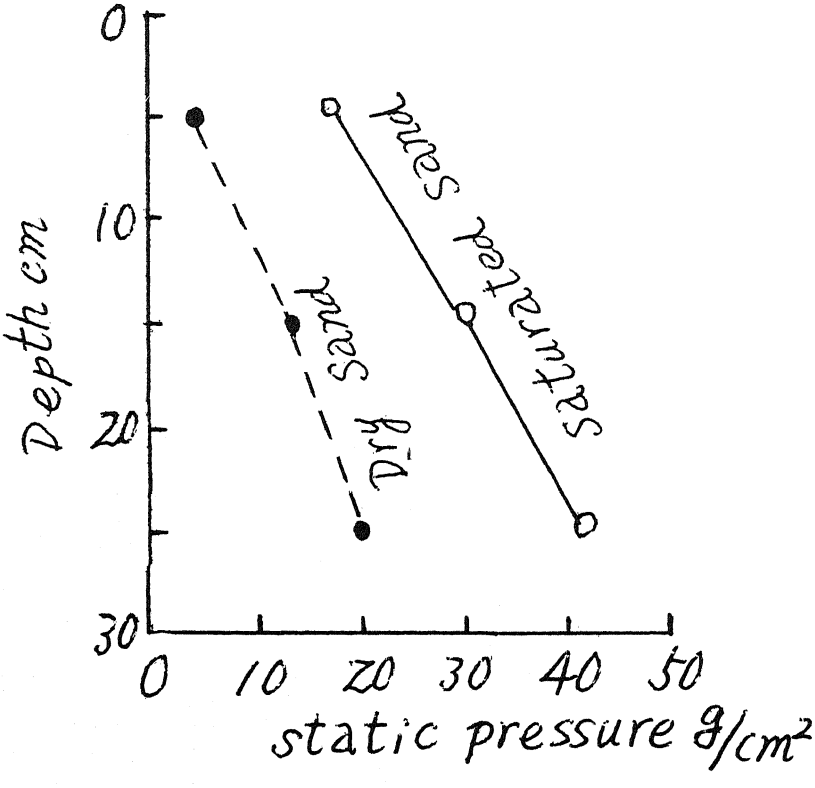
Depth cm
0
10
20
30
0
10
20
30
40
50
static pressure g/cm²
Dry sand
Saturated sand